PRAMANA
— journal of
physics

Vol. 73, No. 5
November 2009
pp. 927–938

Stacking faults and microstructural parameters in non-mulberry silk fibres

S DIVAKARA[1], S MADHU[2] and R SOMASHEKAR[1,*]
[1]Department of Studies in Physics, University of Mysore, Manasagangotri, Mysore 570 006, India
[2]Instrumentation Division, Central Electrochemical Research Institute, Karaikudi 630 006, India
*Corresponding author. E-mail: rs@physics.uni-mysore.ac.in

MS received 6 February 2008; revised 26 May 2009; accepted 11 June 2009

Abstract. We have analysed the broadening of X-ray reflections observed in non-mulberry silk fibres in terms of stacking faults and microstructural parameters using a single-order method and have, with these parameters, developed, for the first time, a procedure to compute the whole pattern of these silk fibres. The essential deviations in the values of microstructural parameters obtained from line profile and whole pattern fitting procedures are discussed in this paper.

Keywords. Stacking; crystallite size; fibres.

PACS Nos 60; 61.10.Nz; 61.41.+e

1. Introduction

Line profile analysis is a powerful method to investigate the microstructural parameters like crystal size ($\langle N \rangle$), lattice strain (g) and stacking faults in polymer materials [1–7]. Currently, several software packages which employ whole powder pattern fitting, to derive the microstructural parameters are commerically available [8–10]. Recently IUCr also conducted Round Robin test to evaluate the different procedures used to determine the crystallite size and lattice strain [11]. All these approaches, in principle, are based on multiple-order method proposed by Warren and Averbach [5]. A majority of these methods employ a single distribution function for the whole pattern from which result an average set of microstructural parameters. In most of the materials examined in the present study, the crystal size is found to change with crystallographic direction. These studies also emphasize upon the importance of line profile analysis [12] and suggest that single-order method is a reasonably good approach to obtain microstructural parameters [13]. Keijser *et al* [14] have also suggested a single-order method employing Voigt function and integral breadth of reflections. For silk fibres and for most of the other natural

fibres, it is very rare to find experimentally, multiple reflections. To overcome this inherent difficulty, a method employing simple, analytical asymmetric function [12] for individual size profile has been proposed in this paper. This method also enables the use of a single crystal size distribution function to account for the whole diffraction pattern which is adequate to quantify stacking faults in materials like metal oxide compounds, but may be inadequate for describing diffraction patterns from silk fibres [15,16]. In this context, we would also like to emphasize that as per the recent Round Robin survey conducted by IUCr [17], Fourier method of profile analysis (single-order method used here) is quite reliable.

This paper describes a method to compute crystallite size, lattice strain and stacking faults in silk fibres, using single-order method, essentially the crystallite size. Using the parameters computed from the single line analysis, the whole pattern observed in three non-mulberry silk fibres Tassar, Muga and Eri has been simulated, and the necessary procedure for doing this is given in this paper. The extent of variation of these parameters obtained from single-order method while refining against the whole pattern refinement is also discussed.

2. The theory

The contribution of crystallite size, lattice strain and stacking faults to a Bragg reflection profile can be written as [10]

$$I_{hkl}(s_{hkl}) = \int_{-\infty}^{\infty} T^{\mathrm{IP}}(nd)\mathrm{e}^{[2\pi i\zeta(nd)]}\mathrm{e}^{[2\pi i\phi(nd)]}\mathrm{e}^{[2\pi ind s_{hkl}]}\mathrm{d}(nd), \tag{1}$$

where T^{IP} is the Fourier transform of instrument profile, $\mathrm{e}^{[2\pi i\zeta(nd)]}$ is the average phase factor due to crystallite size and $\mathrm{e}^{[2\pi i\phi(nd)]}$ is due to lattice distortion and stacking faults. $L = nd$ (with $d = d_{hkl}$) is the column length. This equation can also be written in the form of Fourier series as

$$I_{hkl}(s) = \sum_{n=-\infty}^{\infty} A_{hkl}(n)\cos\{2\pi n d_{hkl}(s - s_0)\}, \tag{2}$$

where $A_{hkl}(n)$ are Fourier coefficients corrected for instrumental broadening using the method of Stokes [18]. Hereafter crystallite size will be referred to in terms of the number of unit cells measured in a direction perpendicular to the Bragg plane with a notation $\langle N\rangle$ and the crystallite size in Å is given by $D_{hkl} = \langle N\rangle d_{hkl}$. These Fourier coefficients $A_{hkl}(n)$ are functions of the size of the crystallite, the disorder of the lattice and stacking fault coefficients, i.e.

$$A_{hkl}(n) = A^s_{hkl}(n) \cdot A^d_{hkl}(n) \cdot A^F_{hkl}(n). \tag{3}$$

Fourier analysis of a Bragg reflection profile must always be performed [19] over the complete cycle of the fundamental from $d(s - s_0) = -1/2$ to $+1/2$, which is rarely possible, experimentally. The analysis was carried out using correction for truncation [13]. For a paracrystalline material like silk fibre, with Gaussian distribution the expression $A^d_{hkl}(n)$ has been given in refs [5,12,13,19,20]. Using the

exponential distribution function for column length an expression for $A^s_{hkl}(n)$ had been reported earlier [12,13].

Warren [19] has given an integral analysis for deformation faults and twin faults in various crystal systems. According to this paper, the shift, broadening and asymmetry of the profile are proportional to these fault densities. Here stacking fault density is defined as the chance of finding a stacking fault between any two adjacent layers causing a Bragg reflection and is denoted by α^d. α^d is normally expressed in percentage and the average number of Bragg planes between stacking faults is given by $1/\alpha^d$. The twin fault probability β is defined as the chance of finding a twin fault between any two adjacent (hkl) layers and the average number of (hkl) layers between twin faults is $1/\beta$. Veltrop *et al* [21] have obtained an equation for Fourier coefficients $A^{\mathrm{F}}_{hkl}(n)$ in terms of the deformation fault (α^d) and twin fault (β) probabilities as

$$A^{\mathrm{F}}_{hkl}(n) = (1 - 3\alpha^d - 2\beta + 3(\alpha^d)^2)^{|(1/2)nd_{hkl}s(L_0/h_0^2)\sigma_{L_0})|}, \tag{4}$$

where $L_0 = h + k + l$, $h_0^2 = h^2 + k^2 + l^2$. σ_{L_0} is assumed to be positive for all reflections studied here.

The whole powder pattern of silk fibre was simulated using individual Bragg reflections represented by the above equations using

$$I(s) = \sum_{hkl}(\omega_{hkl} I_{hkl} - \mathrm{BG}), \tag{5}$$

where ω_{hkl} are the appropriate weight functions for the hkl Bragg reflection. Here s takes the whole range of X-ray diffraction of the sample. BG is an error parameter introduced to correct the background estimation.

Exponential function has been used for the crystallite size distribution and the microstructural parameters are evaluated using eqs (1)–(3). Using these equations the parameters N, α, the background correction factor and g for individual Bragg reflections have been initially computed. For this purpose, SIMPLEX program [22] has been employed. Then the whole pattern fitting was done by introducing weight factors for the individual profiles and also taking into account the average stacking faults derived using eqs (4) and (5) in the final stage of refinement with the whole experimental diffraction data of the sample. Computational procedure is given in the flow chart (see figure 1).

3. Experimental

3.1 *Sample preparation*

Cocoons are the raw material for reel silk fibres. Hence, cocoons of various wild varieties were collected from the germplasm stock of the Department of Sericulture and were reeled following the standard procedure. First, cocoons were cooked in boiling water for 2 min to soften the sericin and later transferred to the water bath at 65°C for 2 min. Then the cocoons were reeled in warm water with the help of a reeling equipment known as Epprouvite. Among the Indian races, there are three different types of raw wild varieties of silk fibres such as Tassar, Muga and Eri.

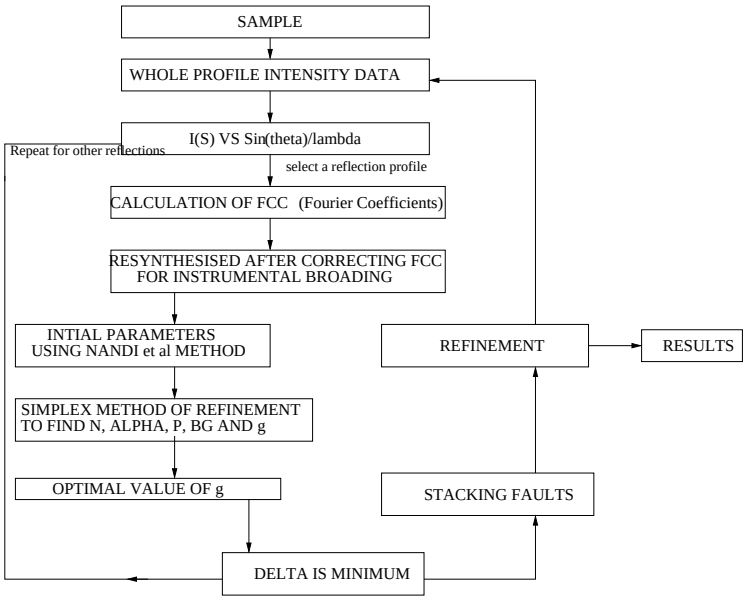

Figure 1. Flow chart for the computation of microstructural parameters.

3.2 *X-ray diffraction pattern*

The XRD diffractograms of the polymer samples were recorded using an X'Pert Pro X-ray diffractometer with Ni filtered, CuKα radiation of wavelength $\lambda = 1.5406$ Å, with a graphite monochromator. The specifications used for the recordings were 40 kV, 30 mA. The samples were scanned in the 2θ range 12–60° with a scanning step size of 0.017°. Figure 2 shows the X-ray diffraction patterns obtained for Tassar, Muga and Eri silk fibres. Here the fibre reflections have been identified using the cell parameters $a = 9.44$ Å, $b = 6.95$ Å, $c = 10.6$ Å and the space group $P2_12_12_1$ [23].

3.3 *Computational procedure*

Equatorial scan of the X-ray diffraction pattern recorded from silk samples was used for the estimation of microcrystalline parameters like crystal size (N) and lattice distortion (g). Further, PEAK-FIT program [24] has been used to extract profiles using Gaussian deconvolution procedure in the overlapping regions and also for background correction. After extraction of the profiles, single-order line profile analysis has been carried out. The instrumental broadening corrections were carried out using Stokes method [18]. For this purpose, ball-milled iron powder was used. These corrections, though relatively small (less than 5%) in polymeric samples compared to metal oxide compounds, were included. The procedure adopted for the computation of the parameters is as follows. Initial values of g and N were obtained

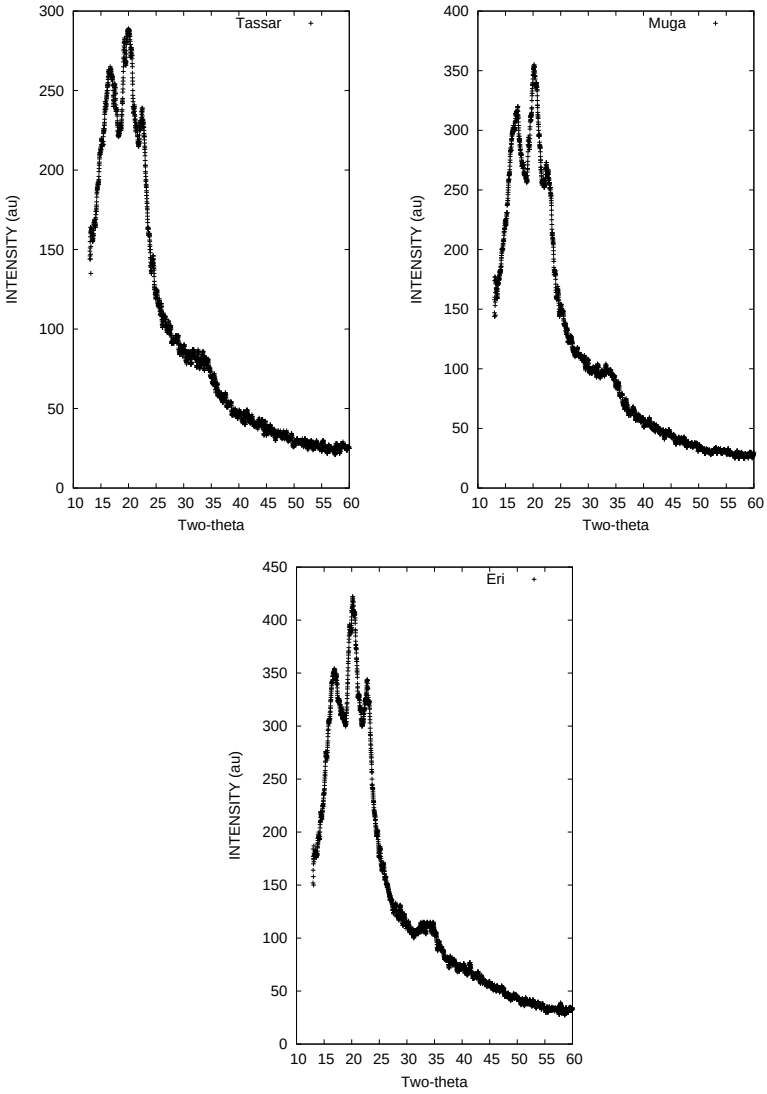

Figure 2. X-ray diffraction patterns obtained for Tassar, Muga and Eri silk fibres for the reflections (0 2 0), (2 1 0), (1 2 1) and (3 2 0)/(2 1 2)/(0 4 0).

using the method of Nandi *et al* [25]. With these values, the equations mentioned earlier in the text, gave the corresponding values for the width of distribution. These are only rough estimates. Hence the refinement procedure must be sufficiently robust to start with such values. The computation is as follows:

$$\Delta = \sqrt{\sum_1^{npt}[I_{hkl}^{\mathrm{cal}} - (I_{hkl}^{\mathrm{exp}} + \mathrm{BG})]^2}/npt, \tag{6}$$

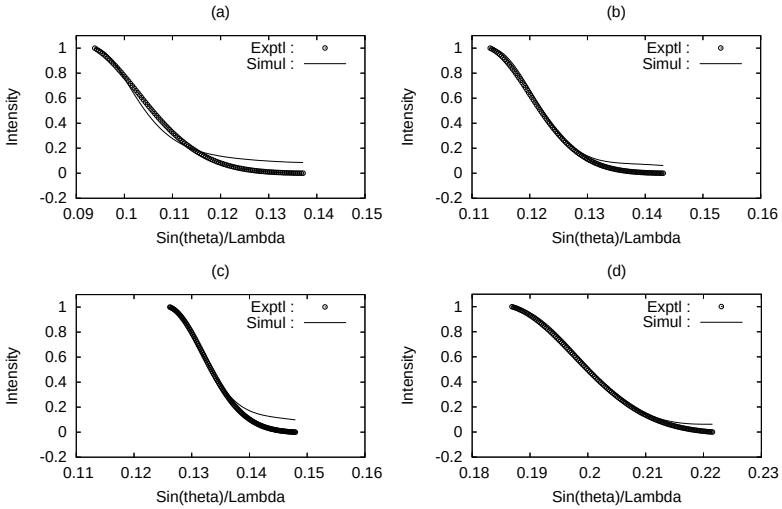

Figure 3. Simulated and experimental profiles for Tassar silk fibre. (**a**) $2\theta = 16.62^\circ$, (**b**) $2\theta = 20.08^\circ$, (**c**) $2\theta = 22.42^\circ$ and (**d**) $2\theta = 33.47^\circ$.

where BG is the error in the background estimation and *npt* is the number of data points in a profile. The values of Δ were divided by half the maximum value of intensity so that it is expressed relative to the mean value of intensities, and then minimized. Further, with these model parameters for individual Bragg reflections, the whole pattern has been simulated and then the refinement against the whole pattern of experimental data has been carried out to compute the final microstructural parameters. For refinement against intensities, the multidimensional minimization algorithm was used [22].

4. Results and discussion

Figures 3–5 show the experimental and simulated intensity profiles for various silk fibres using exponential distribution functions. In all the cases the goodness of the fit was less than 5%. The intensity profiles appear smooth, because we have used interpolation procedure to generate a set of equi-spaced intensity data points from experimental profile. This is essential to compute Fourier coefficients. Comparison between multiple-order and single-order method has been carried out in low density polyethylene (LDPE) and Kevlar^{TM} fibres and appropriate discussions were given in our earlier papers [12,13].

According to Young *et al* [26], the criteria for profile analysis is that a minimum of about 3–4 experimental points must fall within the intensity profile at half height. This condition has been met in our analyses for all the reflections observed in all the samples. The background level was taken as that at which intensity either began to increase with distance from the peak, or became uniform. This was subtracted from all the points and the intensity was assumed to remain zero over the rest of the range required by theory. In the X-ray diffraction intensity profile, we have subtracted

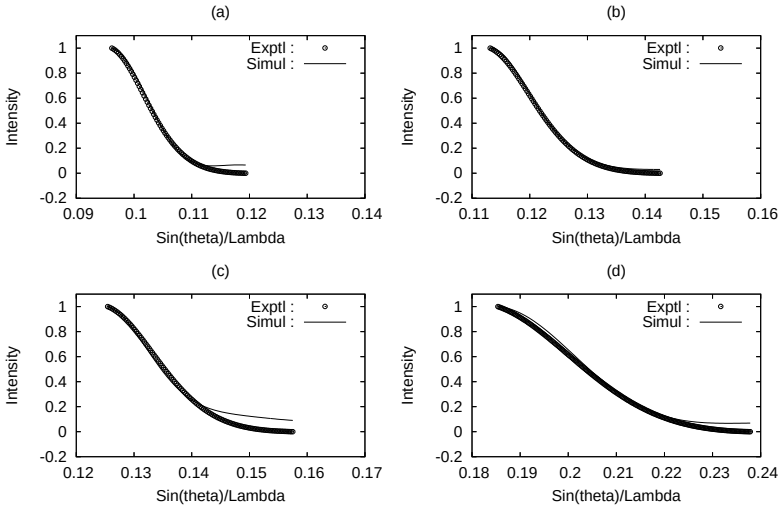

Figure 4. Simulated and experimental profiles for Muga silk fibre. (**a**) $2\theta = 17.04^\circ$, (**b**) $2\theta = 20.08^\circ$, (**c**) $2\theta = 22.28^\circ$ and (**d**) $2\theta = 33.19^\circ$.

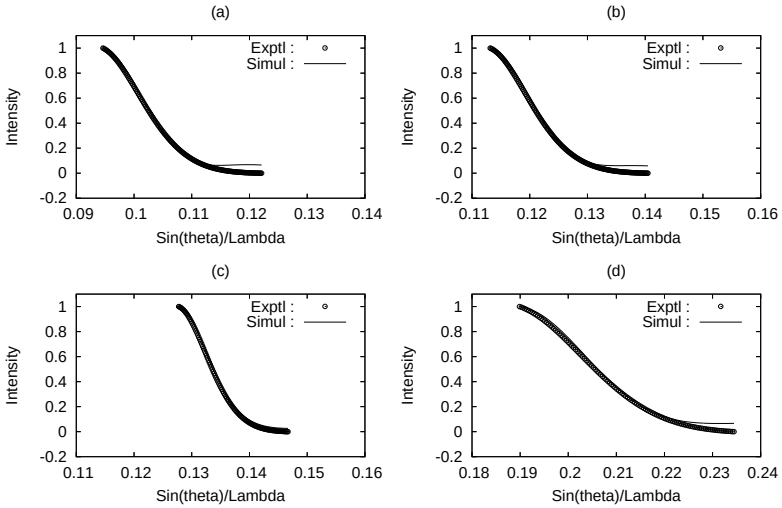

Figure 5. Simulated and experimental profiles for Eri silk fibre. (**a**) $2\theta = 16.76^\circ$, (**b**) $2\theta = 20.08^\circ$, (**c**) $2\theta = 22.70^\circ$ and (**d**) $2\theta = 34.02^\circ$.

only background intensity and not amorphous scattering intensity. A parameter in the refinement process has also been introduced to take care of further error in the estimation of the background as defined in eq. (6). The values of crystallite size, lattice strain, deformation fault probability and twin fault probability are given in table 1. The advantages of single-order line profile analysis is evident in table 1. It is clear that, the crystallite size is different for different Bragg angles (2θ) indicating that the non-spherical distribution of crystallite size is prevalent in these

Table 1. Microstructural parameters of Tassar, Muga and Eri silk fibres using exponential distribution function.

Sample	2θ	g	d_{hkl} (Å)	$\langle N \rangle$	D_{hkl} (Å)	α	α^d	β
	16.62	0.14±0.01	5.3±0.5	5.7±0.6	30±3	0.49±0.05	(1.3±0.1)E-7	(2.8±0.3)E-7
Tassar	20.08	0.09±0.01	4.4±0.4	6.2±0.6	27±3	0.87±0.09	(8.0±0.8)E-7	(2.4±0.2)E-7
silk	22.42	0.07±0.01	3.9±0.4	8.7±0.9	34±3	9.5±0.9	(3.8±0.4)E-5	(9.9±0.1)E-4
fibre	33.47	0.04±0.01	2.7±0.3	6.2±0.6	16±2	2.7±0.3	(7.9±0.8)E-5	(4.2±0.4)E-6
	17.04	0.03±0.01	5.2±0.5	6.0±0.6	31±3	7.0±0.7	(1.6±0.2)E-5	(1.2±0.1)E-4
Muga	20.08	0.03±0.01	4.4±0.4	5.1±0.5	22±2	0.67±0.07	(3.9±0.4)E-8	(1.1±0.1)E-6
silk	22.28	0.09±0.01	3.9±0.4	7.1±0.7	28±3	1.6±0.2	(4.6±0.5)E-6	(2.2±0.2)E-4
fibre	33.19	0.05±0.01	2.7±0.3	4.4±0.4	11±1	2.4±0.2	(4.1±0.4)E-5	(5.1±0.5)E-5
	16.76	0.03±0.01	5.3±0.5	5.2±0.5	27±3	3.3±0.3	(6.0±0.6)E-5	(3.0±0.3)E-7
Eri	20.08	0.04±0.01	4.4±0.4	6.1±0.6	26±3	1.4±0.1	(8.4±0.8)E-8	(7.6±0.8)E-5
silk	22.70	0.02±0.01	3.9±0.4	8.4±0.8	32±3	0.41±0.04	(1.3±0.1)E-9	(4.2±0.4)E-7
fibre	34.02	0.04±0.01	2.6±0.3	5.2±0.5	13±1	2.2±0.2	(3.4±0.3)E-5	(1.3±0.1)E-4

fibres. The variations of crystallite size in different directions are nearly 50% in Tassar, 67% in Muga and 60% in Eri silk fibres.

These parameters have been further refined against the whole pattern recorded from silk fibre by minimizing a term given by an equation similar to eq. (6) but now the summation extends over the whole pattern [eq. (5)]. Subtle changes in these parameters have been observed with the set convergence of 1%. These changes are also given in table 2. The goodness of the fit between simulated and experimental profiles for the three different silk fibres are given in figure 6 along with the difference graph.

The observed variations in the microstructural parameters given in tables 1 and 2 are due to a two-fold refinement. First, the line profile analysis of the extracted profiles from overlapping regions were carried out. This is the standard procedure to compute microstructural parameters. Secondly, the range of overlapping regions do determine the extent of broadening of the reflections. In fact, the broadening may decrease, if the reflections are closeby and hence result in an increase in the crystallite size values. A closer examination of the values in tables 1 and 2 indicates such a result. It is also worth noting that none of the other parameters like lattice strain and stacking fault probabilities varied much during the refinement against the whole pattern data of silk fibres.

To check the reliability of the computed deformation and twin faults, a simple approximate method suggested by Warren [19] has been used here and the expression for the twin fault is given by

$$(2\theta^0_{\mathrm{CG}} - 2\theta^0_{\mathrm{PM}})_{hkl} = -14.6 X_{hkl} \tan\theta \times \beta, \tag{7}$$

where $2\theta^0_{\mathrm{CG}}$ is the centre of gravity of the profile and $2\theta^0_{\mathrm{PM}}$ is the peak maxima. β is the twin fault and X_{hkl} is the constant value which we have taken to be 0.23. For all the three samples the average twin fault probabilities have been computed and the values are 5.2×10^{-7}, 1.2×10^{-6} and 2.7×10^{-7}, which are of the same order of twin fault probability which have been computed by incorporating an appropriate expression in the Fourier coefficients as given in eq. (3). These values are logically reliable and do represent the extent of twin faults present in a fibre in a direction

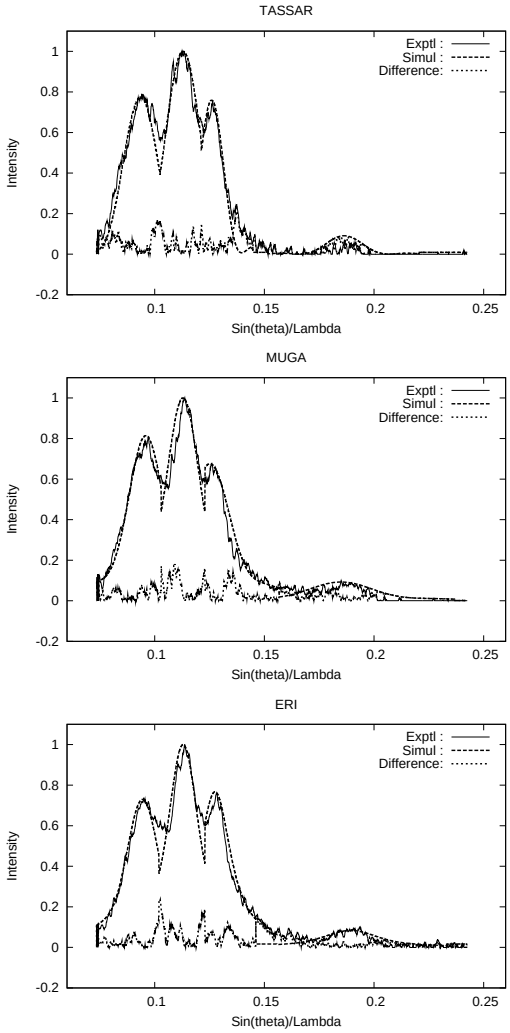

Figure 6. Simulated and experimental profiles for Tassar, Muga and Eri silk fibres along with the diffrences.

perpendicular to the fibre axis. In fact $1/\beta$ is very large in fibres and very small in metal oxide materials. Approximate values of the deformation fault probability α^d have also been estimated by making use of the following expression given by Warren [19]:

$$\frac{1}{\langle D_s \rangle} = \frac{1}{\langle D \rangle} + [(1.5\alpha^d + \beta)/d_{hkl}][\sum_b |L_0|/(u+b)h_0], \tag{8}$$

where u is the unbroadened component, b is the broadened component and $L_0 = 3N + 1$ reflections. We have taken the values of $[\sum_b |L_0|/(u+b)h_0]$ to

Table 2. Microstructural parameters computed from whole pattern refinement.

Sample	2θ	$\langle N \rangle$	ω	BG	g
	16.62	5.7±0.6	0.85±0.09		
Tassar	20.08	6.2±0.6	1.09±0.11	0.01±0.001	0.02±0.002
silk fibre	22.42	8.7±0.9	0.83±0.08		
	33.47	6.2±0.6	0.01±0.01		
	17.04	6.0±0.6	0.88±0.09		
Muga	20.08	5.1±0.5	1.08±0.11	0.001±0.0001	0.11±0.011
silk fibre	22.28	7.1±0.7	0.73±0.07		
	33.19	4.4±0.4	0.01±0.01		
	16.76	5.2±0.5	0.87±0.09		
Eri	20.08	6.1±0.6	1.20±0.12	0.020±0.002	0.13±0.013
silk fibre	22.70	8.4±0.8	0.92±0.09		
	34.02	5.2±0.5	0.01±0.01		

be 0.471 and 1.33 for (2 0 0) and (2 1 0) reflections respectively. Approximate values of deformation fault probability α^d have also been computed for the three silk samples and they turn out to be 2.5×10^{-2}, 7.6×10^{-3} and 3.3×10^{-2} respectively for Tassar, Muga and Eri. A comparison with the deformation fault probability values obtained by Fourier coefficient method (given in tables 1 and 2) indicate that the values are low in fibres because there are too many layers between two successive deformation fault layers. This is due to the fact that there are pockets of crystalline-like order in a matrix of amorphous regions. It is well-known that the Fourier method gives a reliable set of microstructural parameters and it is also shown here that in addition to these values, one can also compute reliable fault probabilities. In this context, it is necessary to draw attention to the fact that as per the survey and results of Round Robin test conducted by IUCr [17] in which the author of the present paper also took part, it is clearly indicated that Fourier method of single-order analysis gives reliable results with regard to crystallite size. Coming to the computation of lattice strain, there is a limited allowed range of values for g. This region is represented by a straight line on graphs of g against $(1/N)^{1/2}$ that includes all the good points [27–29]. The longer the gradient of this line, known as correlation factor, the greater the range of input values which will produce good estimations of size and distortion. Since the present investigation uses Hosemann's paracrystalline model to describe the lattice distortion g in these natural polymers, a plot of g vs. $(1/N)^{1/2}$ will highlight a correlation effect as the theoretical value of the slope is limited to a value of 0.4 [30]. It must be stressed here that the correlation factor is dependent on the error in the estimated crystal size which is deemed acceptable since otherwise, the slope of the straight line representing them will change. The results presented in figure 7 indicate that the experimental points are good points and that we are not measuring the correlation length but the crystallite size. Inaccurate values of g will however, affect the magnitude of the correlation factor.

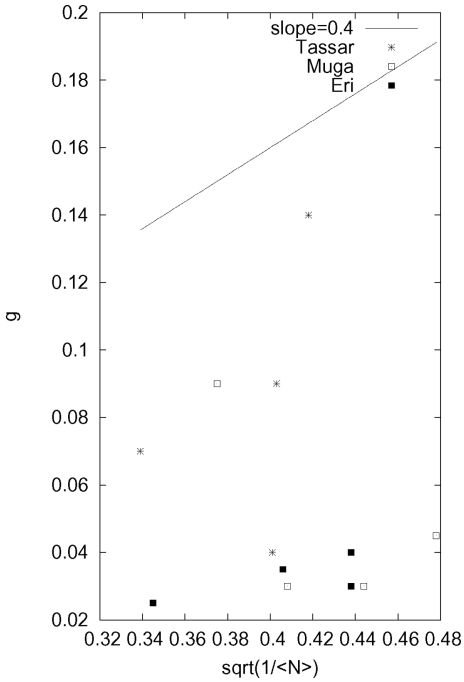

Figure 7. Goodness of the computed g values is given here. Solid straight line is drawn at a slope of 0.4.

The quality of the whole pattern fitting can be appreciated from figure 6 wherein the experimental and modelled patterns are shown by considering twin and deformation faults. Here, the average deformation fault (α^d) is $2.3 \pm 0.1 \times 10^{-5}$, the twin fault ($\beta$) being $5.8 \pm 0.1 \times 10^{-5}$ in non-mulberry silk fibres. A comparison with plastic deformation of Ni powders is done wherein the reported values for α^d and β are 5.0×10^{-5} and 10.0×10^{-5} respectively [10,31,32]. This indicates that the order of magnitude is in reasonable agreement. This comparison has been made just to highlight the fact that the whole pattern analysis carried out here does include the contribution of faulting, crystallite size and lattice strain present in the fibres for the first time.

5. Conclusion

Whole pattern fitting based on single-order line profile analysis for the refinement of experimental diffraction data from fibres in order to compute crystallite size, lattice strain and faulting probabilities proposed here can be regarded as a useful method. An important contribution of such a method is that there are finer changes in the modelled parameters when compared to single-order line profile analysis method, which reduced the systematic error components present in line profile methods. Here, we would like to emphasize that while refining against whole

pattern we have adhered to the basic requirement of Warren's theory that the individual allowed profile range s_0 has been used, which may be absent in the earlier methods.

References

[1] E J Mittemeijer and P Scardi (Eds), *Diffraction analysis of the microstructure of materials* (Springer Verlag, Berlin, Heidelberg, 2003)
[2] R L Snyder, J Fiala and H J Bunge (Eds), *Defect and microstructure analysis by diffraction* (Oxford University Press, 1999)
[3] P Scardi and M Leoni, *J. Appl. Crystallogr.* **39**, 24 (2006)
[4] T R Welberry and B D Butler, *J. Appl. Crystallogr.* **27(3)**, 205 (1994)
[5] B E Warren and B L Averbach, *J. Appl. Phys.* **21**, 595 (1950)
[6] J I Lagford, *Nature (London)* **207**, 966 (1965)
[7] J I Langford, *J. Appl. Crystallogr.* **1**, 131 (1968)
[8] G Ribarik, T Ungar and J Gubicza, *J. Appl. Crystallogr.* **34**, 669 (2001)
[9] Y H Dong and P Scardi, *J. Appl. Crystallogr.* **33**, 184 (2000)
[10] P Scardi and M Leoni, *Acta Crystallogr.* **A58**, 190 (2002)
[11] D Balzar, N Audebrand, M R Daymond, A Fitch, A Hewat, J I Langford, A Lebail, D Louer, O Masson, C N McCowan, N C Popa, P W Stephens and B M Toby, *J. Appl. Crystallogr.* **37**, 911 (2004)
[12] I H Hall and R Somashekar, *J. Appl. Crystallogr.* **24**, 1051 (1991)
[13] R Somashekar, I H Hall and P D Carr, *J. Appl. Crystallogr.* **22**, 363 (1989)
[14] Th H de Keijser, J I Langford, E J Mittemeijer and A B P Vogels, *J. Appl. Crystallogr.* **15**, 308 (1982)
[15] P Scardi and M Leoni, *Acta Crystallogr.* **A57**, 604 (2001)
[16] N C Pope and D Balzar, *J. Appl. Crystallogr.* **35**, 338 (2002)
[17] D Balzar, *IUCr Newsletter* **28**, 14 (2002)
[18] A R Stokes, *Proc. Phys. Soc., London* **61**, 382 (1948)
[19] B E Warren, *X-ray diffraction* (Addison-Wesley, New York, 1969)
[20] B E Warren, *Prog. Met. Phys.* **8**, 147 (1959)
[21] L Velterop, R Delhez, Th H De Keijser, E J Mittemeijer and D Reefman, *J. Appl. Crystallogr.* **33**, 296 (2000)
[22] W Press, B P Flannery, S Teukolsky and Vetterling (Eds), *Numerical recipes* (Cambridge University Press, 1986)
[23] R D B Fraser and T P MavRae, *Conformation in fibrous proteins and related synthetic polypeptides* (Academic Press, New York and London, 1973)
[24] R Chen, K A Jakes and D W Foreman, *J. Appl. Polym. Sci.* **93**, 2019 (2004)
[25] R K Nandi, H R Kuo, W Schlosberg, G Wissler, J B Cohen and B J Crist, *J. Appl. Crystallogr.* **17**, 22 (1984)
[26] R A Young, R J Gerdes and A J C Wilson, *Acta Crystallogr.* **22**, 155 (1967)
[27] R Hosemann, *Colloid. Polym. Sci.* **260**, 864 (1982)
[28] R Hosemann, *Phys. Scr. T1* **142**, (1982)
[29] A M Hindeleh and R Hosemann, *J. Mater. Sci.* **26**, 5127 (1991)
[30] B K Vainshtein, *Diffraction of X-rays by chain molecules* (Elsevier, Amsterdam, 1966)
[31] P G Sanders, A B Witney, J R Weertman, R Z Valier and R W Siegel, *Mater. Sci. Eng.* **A204**, 7 (1995)
[32] P Chatterjee and S P Sen Gupta, *Philos. Mag.* **A81**, 49 (2001)